

## Bond characteristics between FRP and concrete substrates

Houssam Toutanji<sup>1</sup>, Meng Han<sup>2</sup>

<sup>1</sup> Professor and Chair of Civil and Environmental Engineering at the University of Alabama in Huntsville, Huntsville, USA

<sup>2</sup> Construction Engineer at Alabama Department of Transportation, Huntsville, Alabama, USA

**ABSTRACT:** This paper focuses on the development of a fracture mechanics based-model that predicts the debonding behavior of FRP strengthened RC beams. In this study, the existing debonding models based on fracture mechanics are reviewed. Since no approach exists that can exactly predict the failure mode, an extensive database that contains different beam debonding failure modes is formulated. This database includes 351 concrete prisms bonded with FRP plates tested in single and double shear. The existing fracture-mechanics-based models are applied to this database. The properties of adhesive layer used on the specimens in the existing studies were not always available. Thus, the new model's proposal was based on newly conducted pullout tests and data selected from two independent existing studies.

### 1. INTRODUCTION

A new proposed bond strength model was developed based on fracture mechanics approach. The model was verified with fifteen newly conducted pullout tests and twenty four data selected from two existing studies. This model was developed by integrating the shear-slip power law curve. The derivation is completed by combining the integrated results, which represent the interfacial surface energy, and the newly proposed surface energy expression. The current study takes into consideration the shear stiffness of the adhesive layer and develops an equation for calculating the ratio of  $\tau_{max}$  over  $s_o$  based on available data from newly conducted experiments and previously existing studies as well. This ratio is assumed as a function of six material properties: the elastic modulus of the FRP plate  $E_f$ , the thickness of the FRP plate  $t_f$ , the shear modulus of the adhesive layer  $G_a$ , the thickness of the adhesive layer  $t_a$ , the shear modulus of the concrete substrate  $G_c$  and the reference thickness of the concrete substrate  $t_{ref}$ . Only few studies reported the shear modulus and the thickness of the adhesive layer which was found to be important properties in the newly developed models.

### 2. EXPERIMENTAL PROGRAM AND ANALYSIS

Figure 1 shows a simple description of the specimen's configuration. Nine strain gauges were installed on the FRP surface before testing at an interval of 20 mm to monitor the strain distribution along the bond length. Then the specimens were tested under direct shear. Tests were conducted on the 100 kN MTS closed loop electro-hydraulic universal testing machine. Loading and strain information were acquired by the data acquisition system provided by

National Instrument. The concrete substrate was securely fixed on the testing pad connected to the bottom grip and the FRP plate was grabbed by the top hydraulic grip pulling in tension at a rate of 0.5 mm/min with displacement control until failure. The test results are shown in Table 1.

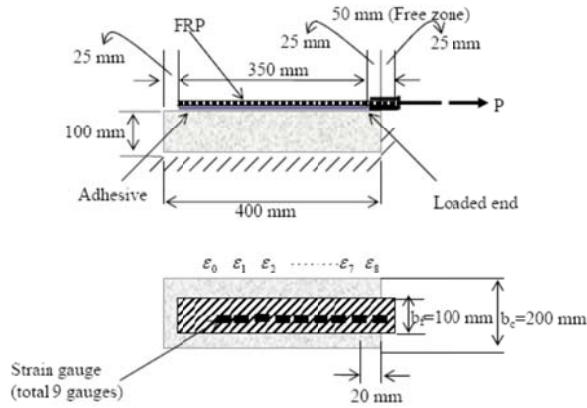


Figure 1 Pure shear experiment-specimen configurations.

Table 1 Details of fifteen newly conducted single lap pullout tests

Spec.	Adh. stiffness	Comp. strength	FRP stiffness	Max. shear	slip	ratio	Fracture energy
	GPa/mm	MPa	kN/mm	MPa	mm		
	$K_a/t_a$	$f'_c$	$E_f t_f$	$\tau_{max}$	$s_0$	$R$	$G_f$ (exp.)
A-2L-F3-Ep1	1.24	70.7	75.24	10.9	0.14	77.86	2.325
A-2L-F3-Ep1	1.28	70.7	75.24	10.42	0.12	86.83	2.233
B-2L-F3-Ep2	1.18	76.3	75.24	10.01	0.11	91	2.075
B-2L-F3-Ep2	1.14	76.3	75.24	9.5	0.13	73.08	2.196
C-2L-F3-Ep2	1.36	40	75.24	9.11	0.084	108.45	1.624
C-2L-F3-Ep2	1.31	40	75.24	9.9	0.09	110	2.228
C-2L-F3-Ep1	1.45	40	75.24	9.41	0.062	151.20	1.881
C-2L-F3-Ep1	1.43	40	75.24	10.05	0.072	139.58	1.841
C-2L-F2-Ep2	7.12	40	71.61	9.64	0.11	87.64	1.249
C-4L-F2-Ep2	0.95	40	143.22	7.11	0.24	29.63	2.888
C-3L-F1-Ep1	1.14	40	104.615	10.24	0.12	85.33	2.186
D-2L-F3-Ep2	0.94	16.3	150.48	5.93	0.151	39.27	2.002
D-2L-F3-Ep2	0.92	16.3	150.48	6.16	0.175	35.2	2.074
D-4L-F3-Ep2	0.94	16.3	150.48	6.44	0.162	39.75	2.045
D-4L-F3-Ep2	0.93	16.3	150.48	6.74	0.167	40.36	2.082

R = the ratio of maximum shear stress over the corresponding slip

As shown in Table 1, all specimens are divided into four groups, A, B, C and D, according to the concrete compressive strength. In each group, the specimens are numbered based on the number of layers of carbon fiber sheets; it is indicated as #L. F# and Ep# represent the type to CFRP and epoxy, respectively.

### 3. NEW MODELS DERIVATIONS

#### 3.1. Maximum shear model

##### 3.1.1 Maximum shear

According to Nakaba et al (2001)'s study, the shear-slip response relationship (Figure 2) can be expressed by the following power law

$$\frac{\tau}{s} = \frac{\tau_{max}}{s_0} \left[ \frac{n}{(n-1) + \left(\frac{s}{s_0}\right)^n} \right], \quad (1)$$

where  $s_0$  is the relative slip between the concrete and the FRP corresponding to a maximum shear stress,  $\tau_{max}$  is the maximum shear stress, and  $n$  is an empirical parameter related to the compressive strength. For concrete with a compressive strength that ranges between 24 MPa and 58 MPa,  $n$  has been determined to be equal to 3. Substituting  $n=3$ , the expression for the shear-slip response becomes

$$\tau = \tau_{max} \frac{s}{s_0} \left[ \frac{3}{2 + \left(\frac{s}{s_0}\right)^3} \right]. \quad (2)$$

The area beneath the curve (Figure 2) is equal to the value of the interfacial fracture energy  $G_f$  (Nakaba et al (2001))

$$G_f = \int_0^{\infty} \tau_{max} \frac{s}{s_0} \left[ \frac{3}{2 + \left(\frac{s}{s_0}\right)^3} \right] ds. \quad (3)$$

The maximum shear stress,  $\tau_{max}$ , and the slip corresponding to the maximum shear stress,  $s_0$ , depend upon on the properties of the concrete-adhesive-composite material system and the slip variation  $ds$ . Thus, after integration, Equation (3) becomes

$$G_f \approx \tau_{max} s_0 (2.214). \quad (4)$$

Assuming that the maximum shear stress,  $\tau_{max}$ , and the corresponding slip,  $s_0$ , have linearly increasing relationships and the ratio of the maximum shear stress,  $\tau_{max}$ , over the corresponding slip,  $s_0$ , is related to the properties of FRP-adhesive-concrete material system,  $R$

$$s_0 = \frac{\tau_{max}}{R}. \quad (5)$$

If the ratio  $R$  can be defined from the properties of material system and substitute Equation (5) into Equation (4), the fracture energy can be described by

$$G_f \approx \tau_{max} s_0 (2.214) = 2.214 \frac{(\tau_{max})^2}{R}. \quad (6)$$

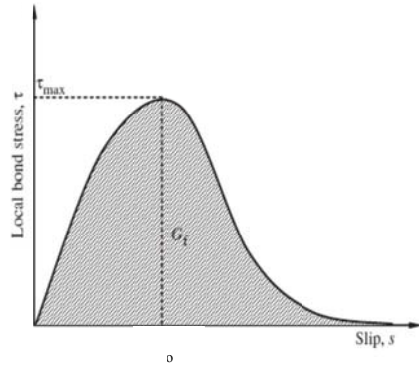


Figure 2 Popvic's expression based on stress-slip relationship between concrete and FRP Nakaba et al. (2001).

Then the interfacial maximum shear can be expressed by

$$\tau_{\max} = \sqrt{\frac{G_f R}{2 \cdot 214}} \quad (7)$$

### 3.1.2 Define the interfacial fracture energy $G_f$

According to the previous work done by Toutanji et al. (2007), the interfacial fracture energy is given by the following bilinear equations

$$G_f = 0.014 f'_c, \text{ when } 0 \leq f'_c \leq 46.2 \text{ MPa} \quad (8)$$

$$G_f = 0.65, \text{ when } f'_c \geq 46.2 \text{ MPa} \quad (9)$$

This expression was derived based on samples with different concrete and FRP mechanical properties but the adhesive characteristics were not considered. All specimens were either failed by concrete shearing or FRP delamination and none of failure by adhesive debonding. Therefore, in order to decide whether this bilinear model is applicable and to describe the interfacial fracture energy very well when soft adhesive is applied, it has to be reevaluated through the data obtained from newly conducted studies (Dai et al. (2005) and Bizindavyi and Neale (1999)). In Figure 3, the triangular dots represent the fracture energy values recorded from the tests and the circle dots represent the values calculated from the bilinear model. It can be seen from this figure that experimental values are commonly much higher than the values calculated from the bilinear model. It was found that those two data groups (triangular and circle dots) would have the straight trend lines with the same slope with one condition: use parameter 0.026 instead of 0.014 in the original bilinear model when the concrete compressive strength is less than 35 MPa as indicated by the one-way arrow in Figure 3.

Thus, the original bilinear model becomes a tri-linear model after this modification. This trilinear model was named  $A(f'_c)$ , function A with respect to the concrete compressive strength  $f'_c$ . Function  $A(f'_c)$  represents the contribution of concrete on the interfacial fracture energy.

$$A(f'_c) = 0.026 f'_c, \text{ when } 0 < f'_c < 35 \text{ MPa} \quad (10)$$

$$A(f'_c) = 0.014 f'_c, \text{ when } 35 \leq f'_c \leq 46.2 \text{ MPa} \quad (11)$$

$$A(f'_c) = 0.65, \text{ when } f'_c \geq 46.2 \text{ MPa} \quad (12)$$

Apparently, the value calculated by function A has a constant different from the tested fracture energy values. This difference is indicated by the two-way dashed arrow in Figure 3. Assume that this difference between trend lines of each data group can be described by the product of functions  $B$  and  $C$ -the effects of FRP characteristics and adhesive characteristics on interfacial fracture energy, respectively-and then fracture energy can be expressed as

$$G_f = A(f'_c) + B(E_f t_f) C(K_a) \quad (13)$$

$$B(E_f t_f) = 0.0946(E_f t_f)^{0.5886} \quad (14)$$

and

$$C(K_a) = 1.0079(K_a)^{-0.2715} \quad (15)$$

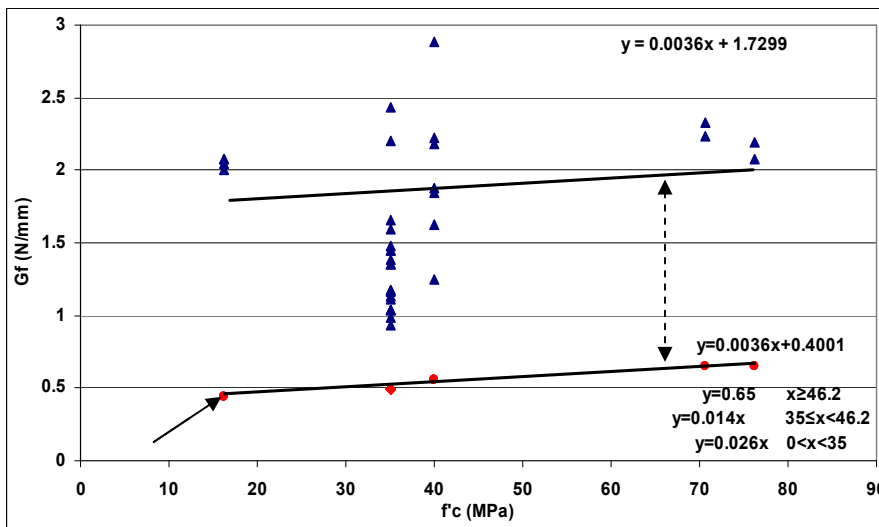


Figure 3 Comparison of the interfacial fracture energy between calculated values from the modified bilinear model and those obtained from tests.

### 3.1.3 Define the ratio $R$ of the maximum shear strength over the corresponding slip

In a standard pure shear debonding test, interface of FRP-concrete material system consists of FRP composite (thickness  $t_f$ ), adhesive layer (thickness  $t_a$ ) and the concrete substrate (reference thickness  $t_{ref}$ ). Each one of them affects the interfacial bond behavior and the ultimate transferable load. Thus, the ratio of  $\tau_{max}$  over  $s_0$  should be expected as a function which includes the characteristics of FRP, adhesive and concrete substrate.

In a pure shear test, the FRP sheet is under tension. This tensile stress in FRP plate is transferred to the concrete surface mainly through shear stresses in the adhesive layer. Thus, tension is the dominant stress in FRP, and shear stress is dominant in both adhesive layer and a very thin layer of concrete substrate adjacent to adhesive. It is reasonable to assume the ratio of  $\tau_{max}$  over  $s_0$  is a function “ $R$ ” with two variations: 1) the tensile stiffness of FRP  $E_f t_f$  and 2) the shear stiffness of both adhesive layer and the very thin layer of concrete adjacent to adhesive layer  $K_0$ . Generally, material shear stiffness is defined as  $K=G/t$ , where  $G$  is material shear modulus,  $t$  is the material thickness. The material system, however, includes adhesive + concrete substrate. According to Dai et al. (2005)’s study,  $K_0$  can be expressed as

$$K_0 = \frac{K_c K_a}{K_c + K_a}, \quad (16)$$

where  $K_a = G_a/t_a$ ,  $K_c = G_c/t_{ref}$ ,  $G_a$  is the shear modulus of the adhesive,  $G_c$  is the shear modulus of the concrete,  $t_a$  is the adhesive thickness, and  $t_{ref}$  is the reference distance in the concrete where it is influenced by the shear stress exerted by the FRP.  $t_{ref}$  was chosen as 15 mm for the best fit in this study. Following Equation (7), the ratio of maximum shear stress over the corresponding slip can be expressed by

$$R = \frac{2.214 \tau_{max}^2}{G_f} \quad (17)$$

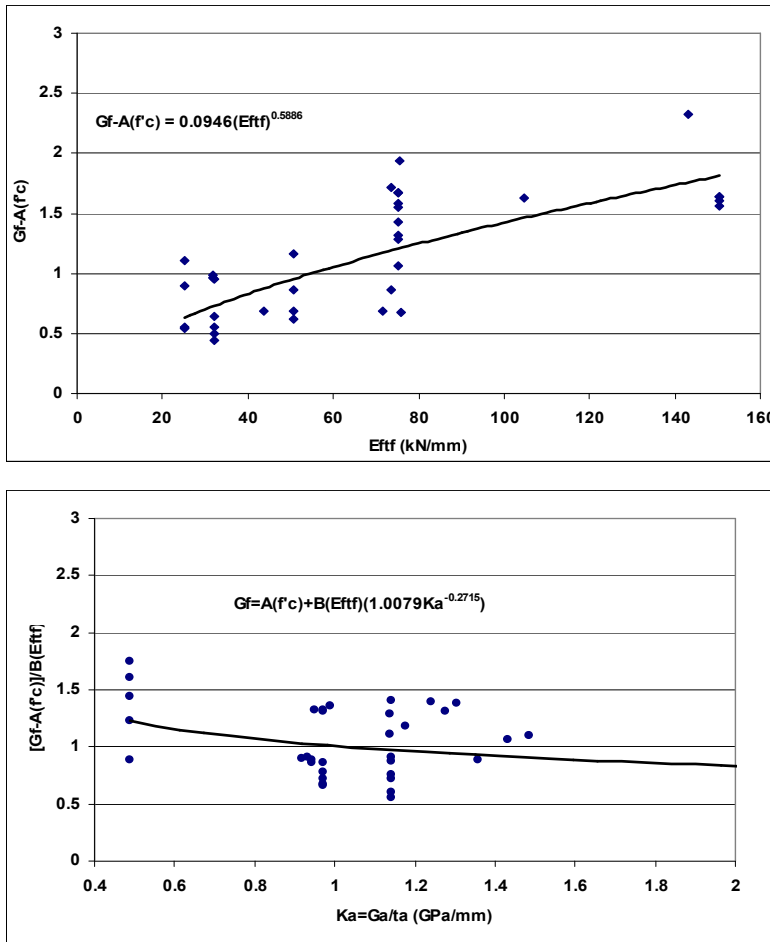


Figure 4 (a) Effect of parameter  $Eftf$  on interfacial fracture energy-function  $B$  and (b) Effect of Adhesive Stiffness  $K_a$  on Interfacial Fracture Energy-function  $C$ .

Substitute the experimental and collected values for maximum shear as shown in Table 1 and predicted interfacial fracture energy into equation (13). Compare the results with the variation of material system shear stiffness  $K_0$  and FRP tensile stiffness  $Eftf$ , as indicated in Figure 5.

$$D(K_0) = 0.0002K_0^{2.1205} \quad (18)$$

$$E(E_f t_f) = 1.6834(E_f t_f)^{-0.0676} \quad (19)$$

Therefore, the ratio of maximum shear stress over the corresponding slip can be expressed by

$$R(K_0, E_f t_f) = D(K_0)E(E_f t_f) \quad (20)$$

Substitute Equations (13) and (20) into Equation (7),  $\tau_{max}$  can be expressed as

$$\tau_{max} = \sqrt{\frac{[A(f'_c) + B(E_f t_f)C(K_a)]R(K_0, E_f t_f)}{2.214}} \quad (21)$$

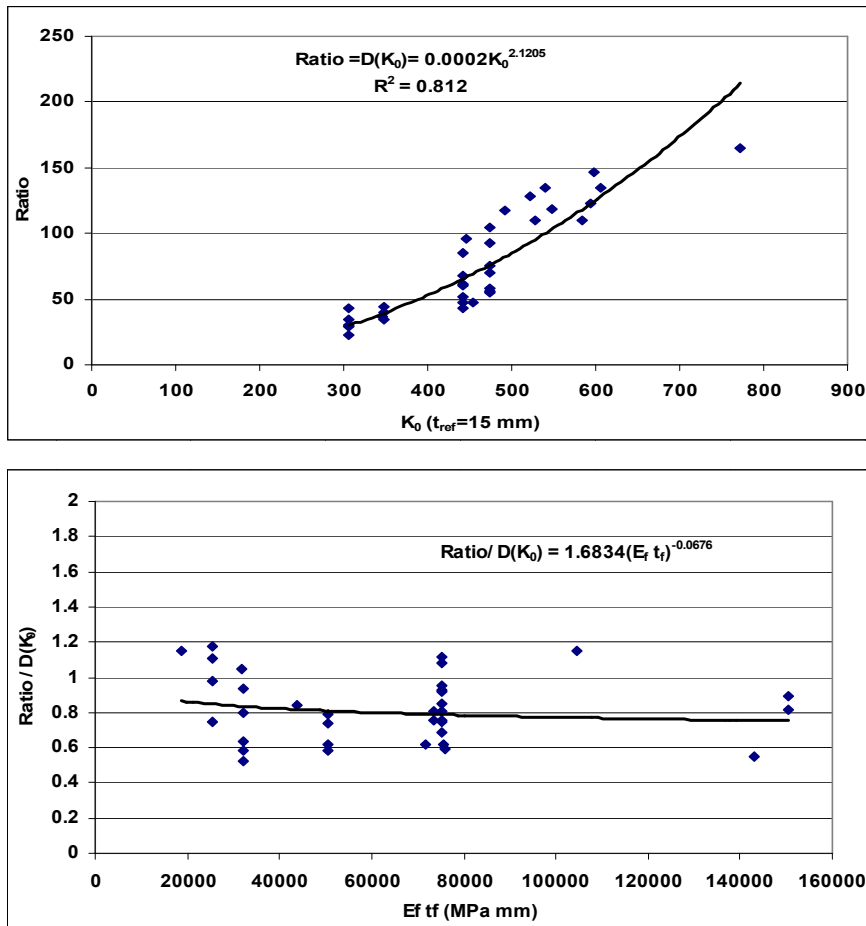


Figure 5 (a) Effect of material system stiffness  $K_0$  on the ratio of maximum shear over the corresponding slip and (b) Effect of fiber-reinforced polymer's stiffness on ratio of maximum shear stress and the corresponding slip.

All available shear stress models including the newly proposed herein have been compared based on the gradually increasing concrete strength in Figure 6. The summary of all existing maximum shear stress models can be found in the references. Most existing models predict that shear strength between the FRP and the concrete substrate highly depends upon the variation of compressive strength of the concrete,  $f'_c$ , for  $f'_c < 35$  MPa (approx.). However, the experiment shows a decreasing acceleration of the maximum shear when the concrete compressive strength

is greater than 35 MPa (approx.). Only the newly proposed model and the model proposed by Ueda and Dai (2005) shows this trend of a decreasing slope for maximum shear. Value-wise, the newly proposed model fits the experimental curve the best, as shown in Figure 6.

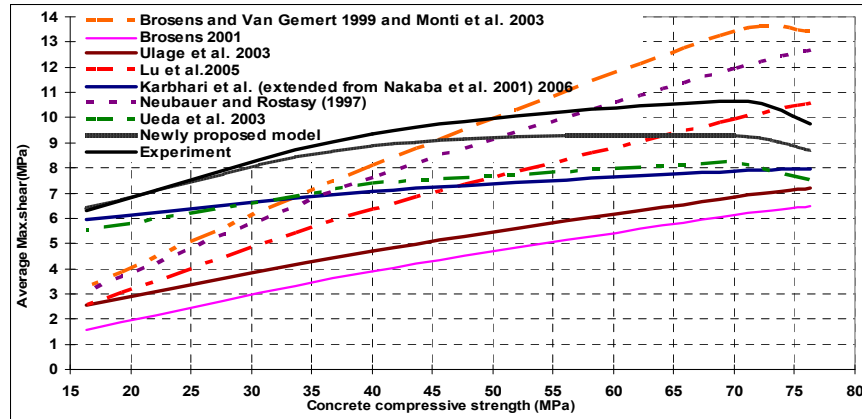


Figure 6 Comparison between the experimental and predicted  $\tau_{max}$  based on the  $f'_c$  variation.

#### 4 CONCLUSIONS

For the purpose of engineering design, a simple maximum shear stress model has been developed by integrating the Nakaba's shear-slip power law curve. Along with the new model's derivation, an expression of interfacial fracture energy was also proposed by taking into consideration the effects of mechanical properties of the adhesive layer, the concrete and the FRP composite. This newly proposed model has characteristics as follows: (1) The maximum bond stress  $\tau_{max}$  increases linearly with  $G_f^{0.5}$ . Since the interfacial fracture energy is independent of the concrete strength after  $f'_c$  is higher than 46.2 MPa, the maximum bond stress is no longer a function of the concrete strength either; (2) With decreasing shear stiffness of the adhesive layer  $K_a$ , both the maximum interfacial bond stress and the shear stiffness of the material system decrease, which leads to an improvement of interfacial fracture energy and the transferable load capacity; (3) With increasing FRP stiffness, the interfacial fracture energy increases and the ratio of maximum shear stress over the corresponding slip decreases slightly. Fifteen pullout tests have been conducted. Comparison between the predicted maximum shear stress and the tested value shows that the proposed model fits the maximum shear distribution the best both trend-wise and value-wise.

#### 5 REFERENCES LIST

- Dai, J, Ueda, T, and Sato, Y. 2005. Development of the nonlinear bond stress-slip model of fiber reinforced plastics sheet-concrete interfaces with a simple method. *Journal of Composites for Construction*, 9: 52-62.
- Bizindavyi, L and Neale, KW. 1999. Transfer lengths and bond strengths for composites bonded to concrete. *Journal. of Composites for Construction*, 3: 153-159.
- Nakaba, K, Kanakubo, T, Furuta, T, and Yoshizawa, H. 2001. Bond behavior between fiber-reinforced polymer laminates and concrete. *ACI Structural Journal*., 98: 359-367.
- Toutanji, H, Saxena, P, Zhao, L, and Ooi, T. 2007. Prediction of interfacial bond failure of FRP-concrete surface. *Journal of Composites for Construction*, 11: 427-432.
- Ueda, T and Dai, J. 2005. Interface bond between FRP sheets and concrete substrates: properties, numerical modeling and roles in member behavior. *Progress in Structural Engineering and Materials*, 7: 27-46.